Supporting Information:

Synthesis of magnetically separable Fe_3O_4-Au-CdS kinked heterotrimers incorporating plasmonic and semiconducting functionalities

Shaghraf Javaid[a], Xiaojie Li[b,c], Fei Wang[a], Wei Chen[a], Yingping Pang[a], Shaobin Wang[b,c], Guohua Jia[a*] and Franca Jones[a*]

a. Curtin Institute of Functional Molecules and Interfaces, School of Molecular and Life Sciences Curtin University, Bentley, Perth WA, 6102, Australia. Email: F.Jones@curtin.ed.au, guohua.jia@curtin.edu.au

b. Department of Chemical Engineering, Curtin University, Bentley, Perth WA, 6102, Australia.

c. School of Chemical Engineering, The University of Adelaide, Adelaide SA 5005, Australia.

*Corresponding author: guohua.jia@curtin.edu.au; F.Jones@curtin.edu.au

X-ray photoelectron spectroscopy (XPS) measurements: The XPS measurements were performed on a Kratos Axis Ultra DLD spectrometer equipped with a monochromatic AlKα (1486.6 eV) irradiation source operating at an X-ray gun power of 150 W. The vacuum pressure of the analysis chamber was maintained at 8 x 10^{-9} Torr or lower throughout the analyses. The scale of binding energy was calibrated for each sample by setting the main line of the C 1s spectrum to 284.8 eV. XPS spectra were collected with 160 eV pass energy for the survey spectra and 40 eV for the high-resolution spectra, respectively. Background subtraction using a Shirley background was applied to all survey and high-resolution spectra. Each high-resolution spectra was fitted with a Gaussian-Lorentzian (70-30 %) line shape with the full-width half maximum (FWHM) constrained to values considered reasonable for each of the element.

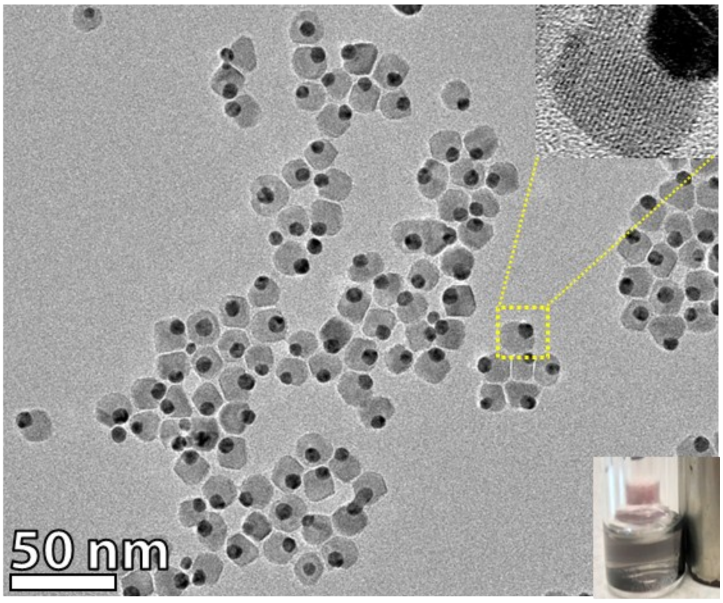

Figure S1. TEM image of Au-Fe_3O_4 dimer seed. Top and bottom right insets show its HRTEM and magnetic separation, respectively.

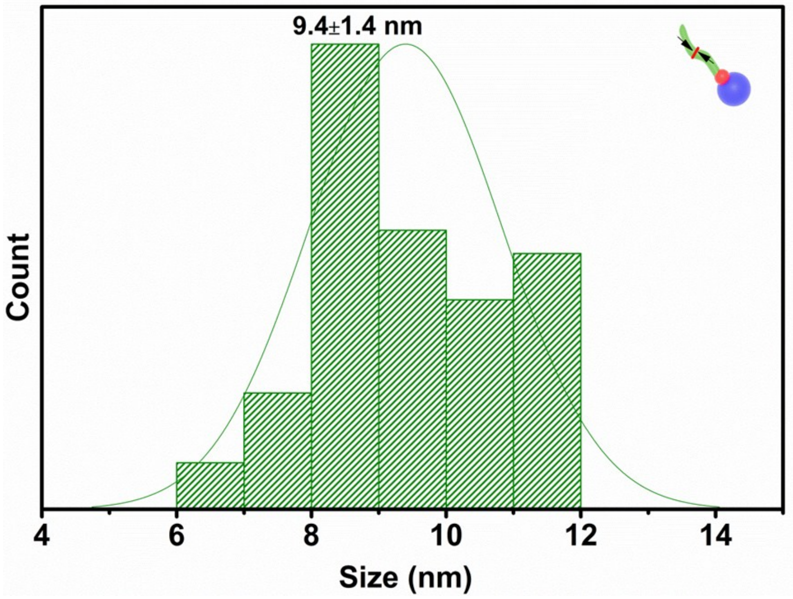

Figure S2. Size distribution curve of the diameter of kinked CdS nanorods.

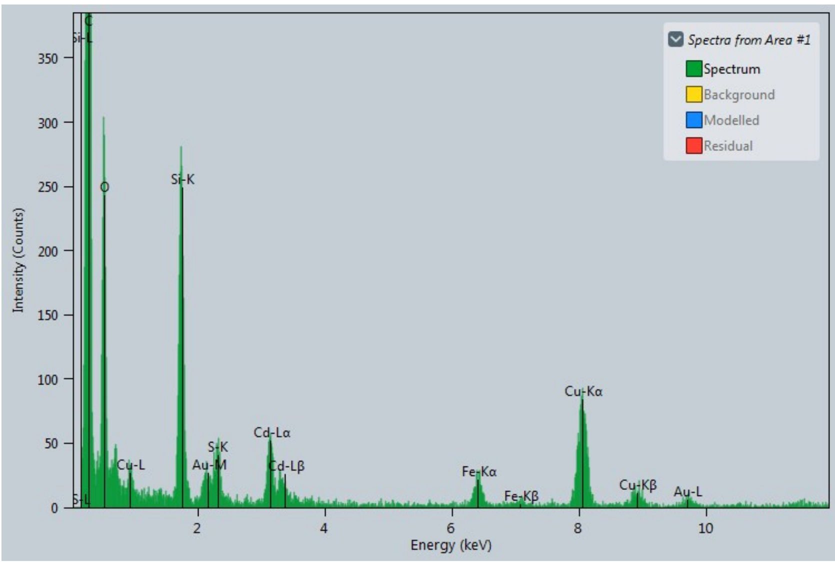

Figure S3. EDS spectra of Fe_3O_4-Au-CdS heterotrimer obtained at 260 °C after 6 mins, corresponding to Figure 1 c1-c2.

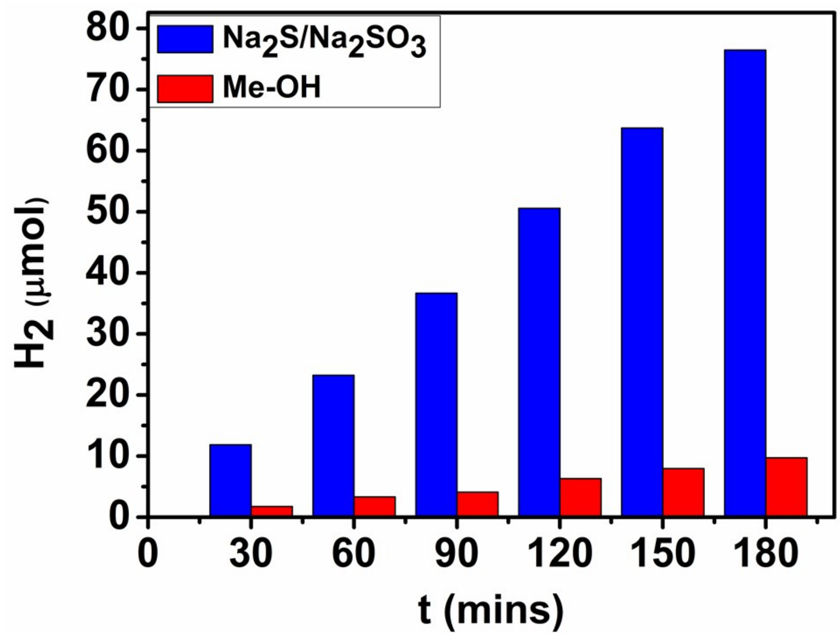

Figure S4. Comparison of the photocatalytic activity of Fe_3O_4-Au-CdS heterotrimer in the presence of Na_2S/Na_2SO_3 and Me-OH as sacrificial agents.

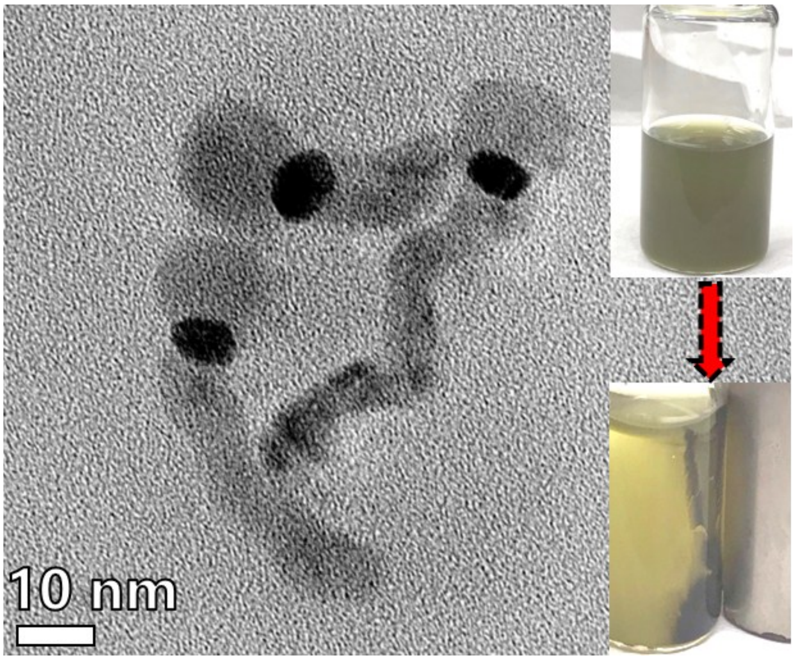

Figure S5. TEM image of the heterotrimer catalyst, Fe_3O_4-Au-CdS with an inset showing its response towards an external magnet.

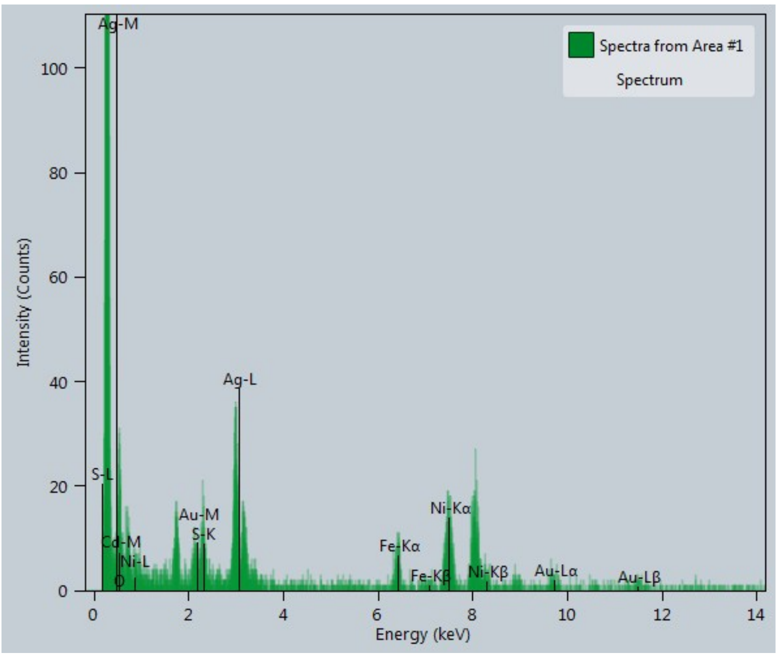

Figure S6. EDS spectra of Fe_3O_4-Au-Ag_2S heterotrimer, corresponding to Figure 6b.

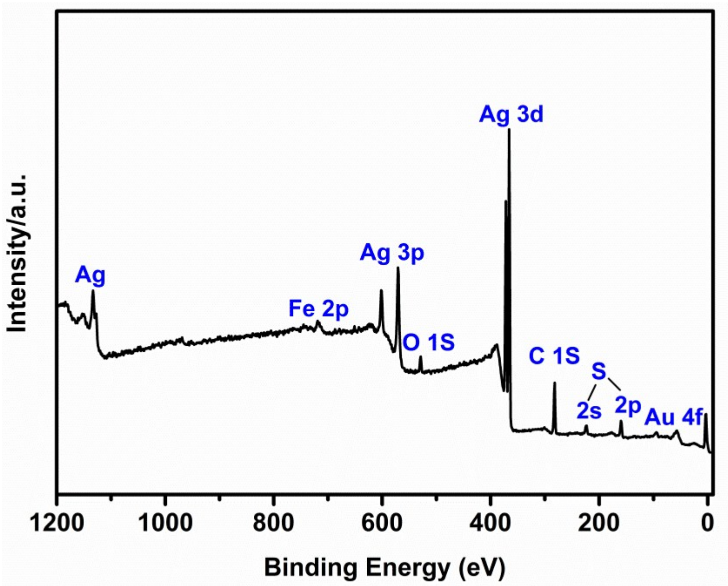

Figure S7. XPS survey spectra of Fe_3O_4-Au-Ag_2S, corresponding to Figure 6h.

Table S1 Photocatalytic activity of Fe_3O_4-Au-CdS in comparison with literature reports.

Hybrid System	**H_2 evolution (μmol)**	**Ref**
Au@TiO_2-CdS	11	[1]
Fe_3O_4-CdS-Ni	18	[2]
In_2O_3/Au/CdS	17.23	[3]
Au NR-TiO_2	11.6	[4]
Fe_3O_4-CdSe-Au	40	[2]
ZnS(CdS/Au)	36.5	[5]
Fe_3O_4-ZnS-Au	12	[2]
Ag-Ag_2S-CdS NPs	40	[6]
Fe_3O_4-Au-CdS	76	Present work

References

1. J. Fang, L. Xu, Z. Zhang, Y. Yuan, S. Cao, Z. Wang, L. Yin, Y. Liao and C. Xue, Au@TiO_2–CdS Ternary Nanostructures for Efficient Visible-Light-Driven Hydrogen Generation, *ACS Appl. Mater. Interfaces*, 2013, **5**, 8088-8092.
2. F. Pang, R. Zhang, D. Lan and J. Ge, Synthesis of Magnetite–Semiconductor–Metal Trimer Nanoparticles through Functional Modular Assembly: A Magnetically Separable Photocatalyst with Photothermic Enhancement for Water Reduction, *ACS Appl. Mater. Interfaces*, 2018, **10**, 4929-4936.
3. D. Ma, J.-W. Shi, D. Sun, Y. Zou, L. Cheng, C. He, Z. Wang and C. Niu, Au Nanoparticle and CdS Quantum Dot Codecoration of In_2O_3 Nanosheets for Improved H_2 Evolution Resulting from Efficient Light Harvesting and Charge Transfer, *ACS Sustain Chem. Eng.* 2019, **7**, 547-557.
4. B. Wu, D. Liu, S. Mubeen, T. T. Chuong, M. Moskovits and G. D. Stucky, Anisotropic Growth of TiO_2 onto Gold Nanorods for Plasmon-Enhanced Hydrogen Production from Water Reduction, *J. Am. Chem. Soc.*, 2016, **138**, 1114-1117.
5. T.-T. Zhuang, Y. Liu, M. Sun, S.-L. Jiang, M.-W. Zhang, X.-C. Wang, Q. Zhang, J. Jiang and S.-H. Yu, A Unique Ternary Semiconductor–(Semiconductor/Metal) Nano-Architecture for Efficient Photocatalytic Hydrogen Evolution, *Angew. Chem. Int. Ed.,* 2015, **54**, 11495-11500.
6. T. Kawawaki, T. Nakagawa, M. Sakamoto and T. Teranishi, Carrier-Selective Blocking Layer Synergistically Improves the Plasmonic Enhancement Effect, *J. Am. Chem. Soc.*, 2019, **141**, 8402-8406.